



Published in final edited form as:

*Kidney Int.* 2014 May ; 85(5): 1068–1077. doi:10.1038/ki.2013.453.

## Podocyte injury enhances filtration of liver-derived angiotensinogen and renal angiotensin II generation

Taiji Matsusaka<sup>1,2</sup>, Fumio Niimura<sup>3</sup>, Ira Pastan<sup>4</sup>, Ayumi Shintani<sup>5,6</sup>, Akira Nishiyama<sup>7</sup>, Iekuni Ichikawa<sup>6,8,9</sup>

<sup>1</sup>Department of Internal Medicine, Tokai University School of Medicine, Isehara, Japan

<sup>2</sup>Institute of Medical Science, Tokai University School of Medicine, Isehara, Japan

<sup>3</sup>Department of Pediatrics, Tokai University School of Medicine, Isehara, Japan

<sup>4</sup>Laboratory of Molecular Biology, Center for Cancer Research, National Cancer Institute, NIH, Bethesda, Maryland, USA

<sup>5</sup>Department of Biostatistics, Vanderbilt University Medical Center, Nashville, Tennessee, USA

<sup>6</sup>Department of Medicine, Vanderbilt University Medical Center, Nashville, Tennessee, USA

<sup>7</sup>Department of Pharmacology, Research Equipment Center, and Second Department of Internal Medicine, Kagawa University School of Medicine, Kagawa, Japan

<sup>8</sup>Tokai University School of Medicine, Isehara, Japan

<sup>9</sup>Department of Pediatrics, Vanderbilt University Medical Center, Nashville, Tennessee, USA

### Abstract

Intrarenal angiotensin II is increased in kidney diseases independently of plasma angiotensin II and is thought to promote progressive deterioration of renal architecture. Here we investigated the mechanism of enhanced renal angiotensin II generation in kidney glomerular diseases. For this, kidney- or liver-specific angiotensinogen gene (*Agt*) knockout was superimposed on the mouse model of inducible podocyte injury (NEP25). Seven days after induction of podocyte injury, renal angiotensin II was increased ninefold in NEP25 mice with intact *Agt*, accompanied by increases in urinary albumin and angiotensinogen excretion, renal angiotensinogen protein, and its mRNA.

**Correspondence:** Taiji Matsusaka, Department of Internal Medicine, Tokai University School of Medicine, 143 Shimokasuya, Isehara, Kanagawa 259-1193, Japan. taijim@is.icc.u-tokai.ac.jp.

#### DISCLOSURE

TM received a research fund from Chugai Pharmaceutical. All the other authors declared no competing interests.

#### SUPPLEMENTARY MATERIAL

**Table S1.** Systolic Blood Pressure (mm Hg).

**Table S2.** Plasma Cystatin C Concentration (ng/ml).

**Table S3.** Representative Values (mean, 95% CI) for the Data Shown in Figures 1 and 4A, and the Body Weight.

**Table S4.** *Agt* Concentration in the Perfusate vs. Arterial Blood.

**Table S5.** Relative *Agt* mRNA Amount.

**Figure S1.** Representative Renal Histology.

**Figure S2.** Representative pictures for nephrin staining.

**Figure S3.** Effects of *Agt* Genotypes on *Agt* mRNA, Protein and Ang II.

**Figure S4.** Focal Leakage of *Agt* Protein in Mouse Models of Focal Segmental Glomerulosclerosis (FSGS).

Supplementary material is linked to the online version of the paper at <http://www.nature.com/ki>

Kidney *Agt* knockout attenuated renal *Agt* mRNA but not renal angiotensin II, renal, or urinary angiotensinogen protein. In contrast, liver *Agt* knockout markedly reduced renal angiotensin II to 18.7% of that of control NEP25 mice, renal and urinary angiotensinogen protein, but not renal *Agt* mRNA. Renal angiotensin II had no relationship with renal *Agt* mRNA, or with renal renin mRNA, which was elevated in liver *Agt* knockouts. Kidney and liver dual *Agt* knockout mice showed phenotypes comparable to those of liver *Agt* knockout mice. Thus, increased renal angiotensin II generation upon severe podocyte injury is attributed to increased filtered angiotensinogen of liver origin resulting from loss of macromolecular barrier function of the glomerular capillary wall that occurs upon severe podocyte injury.

## Keywords

glomerular filtration barrier; nephrotic syndrome; podocyte; proteinuria; renin–angiotensin system

In many forms of kidney disease, pharmacological intervention of angiotensin II (AII) has salutary effects, although plasma AII is generally not elevated. In normal condition, intrarenal AII is above its level in the plasma, and increases further in chronic kidney diseases.<sup>1–9</sup> These findings have collectively formed the prevailing notion that the intrarenal AII is regulated differently from plasma AII, thereby exerting detrimental effects on the renal structure. Among the several mechanisms proposed<sup>7–19</sup> for the increased AII, transcriptional activation of the renal angiotensinogen (*Agt*) gene is thought to play a central role in view of readily demonstrable expression of *Agt* mRNA in the kidney.

*Agt* protein mainly exists in proximal convoluted tubules (S1 and S2 segments). On the other hand, S3 segment contains more *Agt* mRNA than S1 and S2,<sup>20,21</sup> although earlier reverse transcriptase–PCR study by Terada *et al.*<sup>22</sup> showed that both proximal convoluted and straight tubules express *Agt* mRNA. Nevertheless, concurrent increases in *Agt* mRNA and protein seen in renal tissue homogenates have been taken to indicate that transcriptional activation of the renal *Agt* gene causes an increase in renal AII.

In this regard, Pohl *et al.*<sup>21</sup> elegantly demonstrated that *Agt* is a ligand of megalin and that the renal *Agt* protein detectable by immunostaining is taken up from glomerular filtrate by megalin-dependent endocytosis and its localization is distinct from that of *Agt* mRNA.

We recently demonstrated that kidney (proximal straight tubule)–specific *Agt* knockout (KO) mice have markedly decreased renal *Agt* mRNA, but renal *Agt* protein and AII content are unaffected.<sup>23</sup> In contrast, KO of the liver *Agt* gene near completely abolishes renal *Agt* protein and markedly decreases AII contents. Thus, clearly, the liver-derived *Agt* is the major source of renal AII in basal condition. This observation led us to speculate that the functional integrity of glomerular capillary wall as a molecular barrier may determine the renal AII synthesis in progressive glomerular diseases. To test this idea, we analyzed NEP25 mice in which injury can be induced in a podocyte-specific manner by injection of immunotoxin, LMB2.<sup>24</sup> After induction of podocyte injury, renal *Agt* protein and AII increased along with an increase in urinary *Agt* excretion. Moreover, analysis in NEP25 mice carrying mosaic tubular megalin KO revealed that tubular distribution of *Agt* protein in proteinuric state is also completely dependent on megalin. These collectively suggested that

an increase in the leakage of plasma Agt into tubular lumen is the major mechanism of increased renal AII in proteinuric glomerular diseases.

Earlier studies by others, however, reported that in various disease models,<sup>11,25–28</sup> the *Agt* transcription in the proximal tubule is enhanced, raising the possibility that renal *Agt* mRNA may contribute to renal AII synthesis in kidney diseases.<sup>29</sup> This study aims to determine the contribution of the kidney- versus liver-derived Agt to the renal AII generation in glomerular diseases with podocyte injury.

## RESULTS

### Podocyte injury results in massive leakage and renal incorporation of liver-originated Agt protein

We generated NEP25 mice carrying four types of *Agt* genotypes: control intact *Agt* (*Agt<sup>loxP/loxP</sup>*), kidney *Agt* KO (*KAP-Cre:Agt<sup>loxP/loxP</sup>*), liver *Agt* KO (*albumin-Cre:Agt<sup>loxP/loxP</sup>*), and dual *Agt* KO (*KAP-Cre:albumin-Cre:Agt<sup>loxP/loxP</sup>*). In kidney *Agt* KO mice, the *Agt* gene in proximal tubules is mostly disrupted, and renal *Agt* mRNA level is decreased to 14% of that in control or wild-type mice. In liver *Agt* KO mice, the *Agt* gene in the liver is near completely knocked out.<sup>23</sup> The four types of mice were injected with LMB2 (0, 1.25, or 2.5 ng per g body weight (BW)) to induce podocyte injury.

At 7 days after 1.25 or 2.5 ng per g BW of LMB2, all types of mice developed massive proteinuria, with urinary albumin/creatinine (Cr) ratio >60 mg/mg (Figure 1). Analysis in separate mice indicated that blood pressure is not affected by 2.5 ng per g BW of LMB2 in control, kidney, and liver *Agt* KO mice (Supplementary Table S1 online). Cystatin C did not significantly change (Supplementary Table S2 online).

The mice injected with LMB2 did not develop glomerulosclerosis or interstitial fibrosis at this time point (Supplementary Figure S1 online). Nephron staining was diminished, depending on the dose of LMB2 (Figure 2a and Supplementary Figure S2 online). Liver *Agt* KO and dual *Agt* KO mice showed significantly more preserved nephron after 1.25 ng per g BW of LMB2 than control *Agt* mice given the same dose of LMB2. However, after 2.5 ng per g BW of LMB2, mice of all genotypes showed comparably severe nephron loss (Figure 2a). Control and kidney *Agt* KO mice similarly showed early sign of tubulointerstitial damage, including tubule dilatation, tubule apoptosis, and proliferation (Ki67) of tubular and interstitial cells (Figure 2b–e). There was a tendency that liver or dual *Agt* KO mice develop milder tubule apoptosis and Ki67 after 1.25 ng per g BW of LMB2, but more severe tubule dilatation and interstitial Ki67 after 2.5 ng per g BW of LMB2.

In control *Agt* mice, LMB2 markedly and dose-dependently increased renal Agt protein (Figure 3). Kidney *Agt* KO showed similar level of Agt protein at the basal condition and similarly increased Agt after injection of LMB2. In contrast, liver *Agt* KO markedly reduced renal Agt protein in both podocyte-intact and podocyte-injured conditions. Dual *Agt* KO mice showed similar patterns to those of liver *Agt* KO mice.

Immunostaining for Agt paralleled to the result of western analysis. Thus, after injection of LMB2, control and kidney *Agt* KO mice showed similarly intense granular staining in proximal tubule cells (Figure 4). Along the S3 segment, where *Agt* mRNA is intensely expressed, kidney *Agt* KO did not attenuate Agt staining to any appreciable extent. In contrast, liver and dual *Agt* KO mice showed almost no staining after 1.25 ng per g BW of LMB2. After 2.5 ng per g BW of LMB2, although focal Agt staining was discernible along with proteinaceous casts, it was far less than that in control or kidney *Agt* KO mice.

Similar trend was observed in urinary Agt excretion but in a more dramatic manner. Thus, urinary Agt/Cr ratio increased ~300-fold after 1.25 ng per g BW of LMB2, and 1300-fold after 2.5 ng per g BW of LMB2 in control mice (Figure 5). Kidney *Agt* KO mice showed similar patterns to those in control mice. In contrast, Agt/Cr ratio in liver *Agt* KO mice after 1.25 and 2.5 ng per g BW of LMB2 remained at levels of only 5% and 3%, respectively, of those in control mice injected with the same dose of LMB2. Dual *Agt* KO mice showed similarly low urinary Agt. Within control and kidney *Agt* KO mice injected with LMB2, urinary albumin and urinary Agt concentration were significantly correlated ( $r = 0.399$ ,  $P = 0.029$ ; Figure 5).

Separately, the effect of podocyte damage on plasma Agt was studied in NEP25 mice ( $n = 5$ ) with wild-type *Agt* allele. Plasma Agt was, on average,  $2.7 \pm 0.3$   $\mu\text{g/ml}$  before LMB2 injection, and decreased, on average, to  $1.7 \pm 0.3$   $\mu\text{g/ml}$  at 7 days after injection of 2.5 ng per g BW of LMB2 ( $P < 0.05$ ). Hepatic *Agt* mRNA in these mice after LMB2 injection increased to 3.4-fold of that in normal mice without podocyte injury ( $n = 6$ ). We also tested whether Agt within the vascular bed and the interstitial space of the kidney increases after podocyte injury. The blood and interstitial fluid within the kidney were harvested by perfusion. In mice without podocyte injury ( $n = 5$ ), Agt concentration normalized by red blood cell volume in the perfusate was, on average, 1.9-fold of that in the blood collected from the tail artery, likely reflecting that the perfusate contains Agt from the interstitial fluid. In NEP25 mice at 7 days after induction of podocyte injury with 2.5 ng per g BW of LMB2 ( $n = 5$ ), this ratio remained similar, averaging 1.7. These indicate that Agt content in the vascular bed or the interstitial space does not increase after podocyte injury (Supplementary Table S4 online).

These results are taken to indicate that podocyte injury increases glomerular leakage of liver-derived plasma Agt in parallel with albumin, and leads to increase in renal Agt protein. Thus, most renal Agt protein is originated from the liver in glomerular diseases with podocyte injury, a pattern identical to that found in normal condition.

### **Liver Agt KO, but not kidney Agt KO, abrogates the renal AII increase in podocyte injury**

In control mice, LMB2 dose-dependently increased renal AII (Figure 6). Kidney *Agt* KO had no impact on renal AII both before and after LMB2 injection. In contrast, liver *Agt* KO mice, except for one mouse, uniformly showed low level of renal AII in both basal and proteinuric conditions. Dual *Agt* KO mice showed similar low level of renal AII, but no further suppression was observed. The results indicate that in glomerular diseases with podocyte injury, most, if not all, renal AII is originated from the liver-derived Agt.

## Podocyte injury leads to a small increase in renal *Agt* mRNA that is not correlated with the renal AII content

In control *Agt* mice, renal *Agt* mRNA increased dose-dependently after injection of LMB2 (Figure 7a). At the basal condition, kidney *Agt* KO mice showed lower level of *Agt* mRNA than control mice. As KO of the renal *Agt* gene was, at best, partial, residual renal *Agt* gene was activated after LMB2 injection. With 1.25 ng per g BW of LMB2, *Agt* mRNA increased to a level comparable to that of control mice without LMB2, but still remained lower than the level of control mice with the same dose of LMB2. With 2.5 ng per g BW of LMB2, renal *Agt* mRNA increased to a level comparable to that of control mice given the same dose of LMB2. Liver *Agt* KO mice showed similar pattern to control mice, and dual *Agt* KO mice showed similar pattern to kidney *Agt* KO mice.

To examine the site of *Agt* mRNA upregulation, we dissected kidneys from NEP25 mice carrying wild-type *Agt* allele and quantified by real-time reverse transcriptase-PCR. Without podocyte injury, the superficial cortex contains *Agt* mRNA, which is only 6.8% that of the outer medulla, confirming that the S1 and S2 segments contain only small amount of *Agt* mRNA in normal condition. At 7 days after injection of 2.5 ng per g BW of LMB2, *Agt* mRNA increased in both the superficial cortex and the outer medulla (Supplementary Table S5 online), indicating that *Agt* mRNA was upregulated in the region not targeted by KAP-Cre.

Figure 7b shows the relationship between renal *Agt* mRNA and renal AII content after injection of LMB2. The AII content in liver and dual *Agt* KO mice was uniformly low regardless of the *Agt* mRNA level. In contrast, control and kidney *Agt* KO mice showed high renal AII content that was dissociated from renal *Agt* mRNA ( $r = 0.33$ ,  $P = 0.124$ ).

Renal renin mRNA markedly increased in liver and dual *Agt* KO mice (Figure 7c). LMB2 injection led to a slight increase in renin mRNA in control and kidney *Agt* KO mice, and a more marked increase in it in liver and dual *Agt* KO mice. These changes were not parallel with that of renal AII content. Renal *Ace* mRNA was not affected by LMB2 injection in any of the *Agt* genotypes, except for an increase seen with 1.25 ng per g BW of LMB2 in control mice. Besides, there was no significant difference among the *Agt* genotypes (Figure 4d). Similarly, *Ace* mRNA was not in parallel with renal AII content.

Overall, none of these mRNAs in the kidney was in parallel with renal AII content.

## Liver *Agt* KO attenuates sodium (Na) retention after podocyte injury

After injection with 1.25 ng per g BW of LMB2, 94.7% of control or kidney *Agt* KO mice showed readily appreciable ascites and edema in the mesentery that showed transparent jellylike appearance. In contrast, 30.4% of liver or dual *Agt* KO mice showed such phenotypes ( $P < 0.001$ ). After injection with 2.5 ng per g BW of LMB2, 91.6% of control or kidney *Agt* KO mice developed massive ascites, some with leakage through the abdominal wall, and edema involving the intestinal wall. In contrast, 11.8% of liver or dual *Agt* KO mice showed such phenotypes ( $P < 0.001$ ). These were not, however, reflected by the body weight gain, probably because of leakage of ascites through the abdominal wall and appetite loss caused by intestinal edema. The severer edema was reflected by lower urinary Na

secretion that was discernible when urinary Na concentration was normalized by urinary albumin concentration (Figure 8). In all genotypes of mice injected with LMB2, urinary Na/albumin ratio was inversely correlated with renal AII content (Figure 8d).

## DISCUSSION

Podocyte injury markedly increased renal AII content. Upon podocyte injury, renal AII increased, on average, to 1200 fmol/g in control *Agt* mice, a level 9 times of that found without podocyte injury, and 35 times the blood content in normal mice (data not shown). This marked increase was accompanied by increases in urinary *Agt* and renal *Agt*. These were all abolished by liver *Agt* KO, but not by kidney *Agt* KO, thus demonstrating unequivocally that renal AII that increases upon loss of molecular barrier function of the glomerular capillary wall originates from liver-derived *Agt*. As *Agt* content in the vascular and interstitial spaces remained unchanged after podocyte injury, the increased renal AII is likely generated from filtered *Agt*, although we did not directly test this notion. Apart from this is the fact that podocyte injury also enhanced renal *Agt* transcription. This occurred even in kidney *Agt* KO mice, resulting in elevation of renal *Agt* mRNA to a level comparable to that in control *Agt* mice after 2.5 ng per g BW of LMB2. Nevertheless, several lines of evidence indicate that the increased renal *Agt* mRNA has little contribution to the enhanced renal AII generation. First, after 1.25 ng per g BW of LMB2, kidney *Agt* KO mice showed attenuated renal *Agt* mRNA, but renal AII was similarly elevated to that in control *Agt* mice injected with the same dose of LMB2. Second, there was no correlation between renal *Agt* mRNA and renal AII in control and kidney *Agt* KO mice injected with LMB2. Third, liver *Agt* KO near completely abolished the otherwise anticipated renal AII increase regardless of the renal *Agt* mRNA level.

Notably, renin mRNA is increased by some 50 times in liver *Agt* KO mice compared with control *Agt* mice. Despite this marked renin mRNA increase, renal AII was suppressed in liver *Agt* KO mice both with and without podocyte injury. These indicate that renin is not the rate-limiting factor for renal AII generation in these conditions. Instead, availability of the substrate, *Agt*, determines the renal AII synthesis.

The present study investigated the renin–angiotensin system in kidneys with podocyte injury. Several studies reported renal AII increases along with small upregulation of renal *Agt* mRNA in animal models. The magnitude of renal *Agt* mRNA upregulation found in those studies, however, was uniformly small, for example, 1.2–1.5-fold in AII infusion,<sup>27,28,30</sup> 1.47-fold in a model of heart failure,<sup>31</sup> 2.0-fold in a uninephrectomy model,<sup>26</sup> and 2.6-fold in a spontaneous hypertensive rat model.<sup>25</sup> These are either comparable to, or less than, the magnitude observed in this study. Given the constitutively low renal AII in liver *Agt* KO mice with podocyte injury, it appears that an approximately twofold increase in renal *Agt* mRNA may not be sufficient to increase renal AII to an appreciable level.

Our previous study indicates that, in normal mice with intact podocytes, approximately a half of urinary *Agt* is derived from *Agt* synthesized in the proximal tubule, whereas this demonstrated that the massive urinary *Agt* seen in mice with podocyte injury is mostly derived from the liver. In concert with the latter notion, a clinical study by van den Heuvel *et*



*al.*<sup>32</sup> found that urinary Agt and albumin were correlated in diabetic patients. However, somewhat different observation was made by Nishiyama *et al.*<sup>33</sup> They noted dissociation between the magnitude of urinary Agt excretion and that of proteinuria in glomerular diseases. Thus, urinary Agt was increased in patients with IgA nephropathy, but not in those with minor glomerular abnormalities, although the latter group had more marked proteinuria. The observed difference in the behavior of urinary protein versus Agt may best be explained by the difference in the electrical charge of the two similar-size molecules, that is, negatively charged albumin versus almost-neutral Agt. Thus, in glomerular diseases with minor barrier defect, that is, loss of charge selectivity, such as in minimal change disease, marked albuminuria develops whereas glomerular leak of Agt is hardly affected. In contrast, in glomerular diseases with severe barrier dysfunction, that is, loss of molecular size selectivity, angiotensinogenuria develops. In the latter condition, which is clinically characterized by nonselective proteinuria, glomeruli are at the risk of progressive deterioration, in which pharmacological inhibition of AII has often a salutary effect.

In a recent study, Nakano *et al.*<sup>34</sup> studied to visualize glomerular permeability of Agt, using *in vivo* multiphoton imaging technique, and found it to be low in normal C57BL/6 mice. In addition, glomerular sieving coefficient of Agt was found not to be significantly increased in Munich–Wistar–Frömter rats, a model of glomerulosclerosis. The discordant results may reflect different nature of podocyte injury. The proteinuria in Munich–Wistar–Frömter rats is characterized by selective albuminuria, whereas that in NEP25 mice is nonselective.<sup>35</sup> The model used in this study represented relatively severe conditions with prominent nonselective proteinuria. We also observed local enhancement of renal Agt staining in NEP25 mice given 0.625 ng per g BW of LMB2, and in a model of adriamycin nephropathy, as well as in another slowly progressive focal segmental glomerulosclerosis model, that is, transgenic mice expressing mutant  $\alpha$ -Actinin-4 (Supplementary Figure S4 online). These suggest that podocyte injury that later leads to glomerulosclerosis involves leakage of Agt.

Liver *Agt* KO mice showed milder glomerular injury after a low dose (1.25 ng per g BW) of LMB2, but more severe tubule injury after a high dose (2.5 ng per g BW) of LMB2. These likely reflect the effects of low blood pressure and hypoperfusion, respectively. Yet, it is theoretically possible that the transcription of *Agt* in the kidney is increased in liver *Agt* KO mouse, thereby accounting for the somehow worsened tubular injury, although kidney *Agt* KO showed no protective effect. Notably, liver *Agt* KO markedly attenuated the severe edema that otherwise developed in immunotoxin-treated NEP25 mice. This attenuation was in parallel with the observed higher Na excretion in *Agt* KO mice than that in control or kidney *Agt* KO mice. As liver *Agt* KO dampens not only renal but also circulating AII, these effects of liver *Agt* KO on Na excretion are attributed to either loss of renal II or removal of AII from the circulation, or a combination thereof. With regard to the mechanism of edema formation in nephrotic syndrome, it is now believed that local, as opposed to systemic, mechanism exists within the kidney for salt retention.<sup>36</sup> In this regard, this study has provided an attractive and plausible explanation, that is, enhanced production of AII in kidneys with podocyte damage. Further study is necessary to establish the role of so-locally produced AII.

In conclusion, this study indicated that the enhanced renal AII in severe podocyte damage is because of the loss of the barrier function of the glomerular capillary wall allowing massive influx of the AII precursor plasma Agt, and not to transcriptional activation of the *Agt* gene in renal cells.

## MATERIALS AND METHODS

### Animal experiments

Kidney (proximal tubule)-specific *Agt* KO mice, which carry *KAP-Cre* and *Agt<sup>loxP/loxP</sup>*, and liver (hepatocyte)-specific *Agt* KO mice, which carry *albumin-Cre* and *Agt<sup>loxP/loxP</sup>*, were previously reported.<sup>23</sup> In the kidney of kidney *Agt* KO mice, *Agt* mRNA decreases to 14% of baseline after treatment of testosterone. In the kidney of liver *Agt* KO mice, *Agt* mRNA is almost completely abolished. These lines were mated with *NEP25* mice, and the following four kinds of mice were generated and used for this study: namely, *NEP25/control Agt* (carrying *NEP25/Agt<sup>loxP/loxP</sup>*), *NEP25/kidney Agt* KO (*NEP25/ KAP-Cre/Agt<sup>loxP/loxP</sup>*), and *NEP25/liver Agt* KO (*NEP25/albumin-Cre/Agt<sup>loxP/loxP</sup>*). As *KAP* promoter is androgen dependent, only male mice treated with testosterone (50 µg per g BW subcutaneous, 5 times) were used for the experiments.

To induce podocyte injury, LMB2 (1.25 or 2.5 ng per g BW) was intravenously injected.<sup>24</sup> On day 7, mice were killed and kidneys were harvested. For AII, protein, and mRNA assays, kidneys were frozen in liquid nitrogen. Before LMB2 injection and also before killing, 24-h urine was collected and the concentrations of creatinine, albumin, and Agt protein were determined as previously described.<sup>23</sup>

### Morphometric analyses

Nephrin was stained and semiquantified as previously reported.<sup>37</sup> Tubule dilatation was semiquantified using scores from 0 (no dilatation) to 4 (most extensive and severe dilatation) in 12 visual fields on periodic acid–Schiff–stained 2 µm sections, and average scores were calculated. Apoptotic cells were stained by TUNEL (TdT-mediated dNTP nick end labeling) method using a kit (Takara Bio, Otsu, Shiga, Japan). The TUNEL-positive cells in tubules or in tubular lumen were counted in the whole cortex and outer medulla, and the density was calculated. Ki67 was stained using a monoclonal antibody (Leica Microsystems, Tokyo, Japan). The Ki67-positive cells were counted separately within and outside tubules in the whole cortex and outer medulla, and the density was calculated.

### Assays for renal AII content, renal and urinary Agt protein, and mRNAs

Kidneys were cut in half and immediately frozen in liquid nitrogen and stored at –80 °C. Renal AII content was determined by radioimmunoassay as previously described.<sup>23</sup>

Western analysis for Agt was performed as previously described. Under denatured conditions, 5 µg of renal protein from each mouse was separated in five sodium dodecyl sulfate–polyacrylamide gels each containing a common internal control sample. They were transferred onto polyvinylidene difluoride membrane. Agt protein was detected with rabbit anti-Agt antibody (Immuno-Biological Laboratories, Fujioka, Japan) diluted at 1:400 with



Can Get Signal immunoreaction enhancer solution (Toyobo, Tokyo, Japan). Actin was detected with rabbit monoclonal anti- $\beta$ -actin antibody (Cell Signaling Technology, Tokyo, Japan) diluted at 1:1000. Densitometric analysis was performed using CS analyzer (Atto, Tokyo, Japan).

Real-time reverse transcriptase-PCR was performed for *Agt*, renin, *Ace* mRNA, and 18S rRNA using TaqMan primer probe sets and StepOne Real Time PCR Systems (Life Technologies Japan, Tokyo, Japan). Relative amount for *Agt*, renin, and *Ace* mRNA was determined by the CT method.

Plasma and urinary Agt was determined by enzyme-linked immunosorbent assay (ELISA; IBL, Fujioka, Gumma, Japan). The sensitivity of the ELISA kit is  $\geq 0.03$  ng/ml. The specificity was verified by negative detection of Agt in plasma or urine from whole body *Agt* KO mice. For the assays, plasma samples were diluted 1000-fold, and urine samples from control and kidney *Agt* KO mice after LMB2 injection were diluted 9100-fold. Other urine samples were diluted 13-fold.

### Statistical analysis

Data for urinary albumin/Cr ratio and urinary Agt/Cr ratio were analyzed by general linear model after logarithmic transformation to improve normality of residuals. For analyses where heteroscedasticity was observed even after transforming outcome variables, data for Agt protein, renal AII, nephrin index, tubule dilatation, tubule apoptosis, tubular Ki67, and interstitial Ki67 were analyzed by generalized estimating equation method. *Agt* mRNA was analyzed by general linear model using dose of LMB2 as a continuous covariate to examine linear dose-response association and the model included cross-product terms between LMB2 and genotypes to statistically assess whether the effect of LMB2 differed by genotypes. As the interaction between LMB2 and genotypes was not significant, the cross-product terms were excluded from the general linear model, resulting in a common slope for all genotypes, that is, a single  $\beta$ -coefficient to quantify the effect of LMB2 for all genotypes. Renin/18S RNA was analyzed by generalized estimating equation after square root transformation. *Ace*/18S RNA was analyzed by general linear model after square root transformation.

For systolic blood pressure and plasma cystatin C concentration, values before and after LMB2 were compared by Wilcoxon signed-rank test in each group. Difference between genotype was analyzed using Mann-Whitney *U*-test. The *P*-values were corrected by Holm's method in order to minimize inflation of type I error due to multiple comparisons. These are expressed by mean  $\pm$  95% confidence interval.

Plasma Agt in NEP25 mice was expressed by mean  $\pm$  95% confidence interval and the values before and after podocyte injury were compared by paired *t*-test.

Association between urinary (U)-albumin and U-Agt in control or liver *Agt* KO mice injected with LMB2 (Figure 5b) was evaluated by calculating Spearman's rank correlation coefficient after logarithmic transformation. To highlight the low U-Agt in liver and dual *Agt* KO mice observed in the study, data for U-Agt and U-albumin were plotted linearly in Figure 5b.

Association between renal AII and U-Na/albumin after LMB2 (Figure 8d) was evaluated by calculating Spearman's rank correlation coefficient.

Incidence of ascites and edema was compared between control and kidney *Agt* KO mice versus liver and dual *Agt* KO mice using the  $\chi^2$  test.

Values were regarded as significant at two-sided  $P < 0.05$ .

## Supplementary Material

Refer to Web version on PubMed Central for supplementary material.

## ACKNOWLEDGMENTS

We acknowledge Ms Shiho Imai and Ms Chie Sakurai for excellent technical assistance and Ms Tanaka for administrative assistance. This study was supported by Grant-in Aid for Scientific Research of Japan Society for the Promotion of Science, MEXT, MEXT-Supported Program for the Strategic Research Foundation at Private Universities (2009-2013), Project Research (2010–2011) in Tokai University, Grant-in-Aid from the American Heart Association (12GRANT11630000), and in part by the Intramural Research Program of the NIH, National Cancer Institute, Center for Cancer Research.

## REFERENCES

1. Navar LG, Nishiyama A. Why are angiotensin concentrations so high in the kidney? *Curr Opin Nephrol Hypertens* 2004;13: 107–115. [PubMed: 15090867]
2. Kobori H, Nangaku M, Navar LG et al. The intrarenal renin-angiotensin system: from physiology to the pathobiology of hypertension and kidney disease. *Pharmacol Rev* 2007;59: 251–287. [PubMed: 17878513]
3. Pendergrass KD, Averill DB, Ferrario CM et al. Differential expression of nuclear AT1 receptors and angiotensin II within the kidney of the male congenic mRen2. Lewis rat. *Am J Physiol Renal Physiol* 2006;290: F1497–F1506. [PubMed: 16403834]
4. Siragy HM, Carey RM. Role of the intrarenal renin-angiotensin-aldosterone system in chronic kidney disease. *Am J Nephrol* 2010;31: 541–550. [PubMed: 20484892]
5. Bader M, Ganten D. Update on tissue renin-angiotensin systems. *J Mol Med (Berl)* 2008;86: 615–621. [PubMed: 18414822]
6. Li J, Zhou C, Yu L et al. Renal protective effects of blocking the intrarenal renin-angiotensin system. *Hypertens Res* 1999;22: 223–228. [PubMed: 10515446]
7. Largo R, Gomez-Garre D, Soto K et al. Angiotensin-converting enzyme is upregulated in the proximal tubules of rats with intense proteinuria. *Hypertension* 1999;33: 732–739. [PubMed: 10024337]
8. Takase O, Marumo T, Imai N et al. NF-kappaB-dependent increase in intrarenal angiotensin II induced by proteinuria. *Kidney Int* 2005; 68: 464–473. [PubMed: 16014023]
9. Ruiz-Ortega M, Gonzalez S, Seron D et al. Ace inhibition reduces proteinuria, glomerular lesions and extracellular matrix production in a normotensive rat model of immune complex nephritis. *Kidney Int* 1995; 48: 1778–1791. [PubMed: 8587237]
10. Ibrahim HN, Hostetter TH. The renin-aldosterone axis in two models of reduced renal mass in the rat. *J Am Soc Nephrol* 1998;9: 72–76. [PubMed: 9440089]
11. Anderson S, Jung FF, Ingelfinger JR. Renal renin-angiotensin system in diabetes: functional, immunohistochemical, and molecular biological correlations. *Am J Physiol* 1993;265: F477–F486. [PubMed: 8238377]
12. Hsieh TJ, Zhang SL, Filep JG et al. High glucose stimulates angiotensinogen gene expression via reactive oxygen species generation in rat kidney proximal tubular cells. *Endocrinology* 2002; 143: 2975–2985. [PubMed: 12130563]

13. Singh R, Singh AK, Leehey DJ. A novel mechanism for angiotensin II formation in streptozotocin-diabetic rat glomeruli. *Am J Physiol Renal Physiol* 2005; 288: F1183–F1190. [PubMed: 15701818]
14. Taniguchi M, Kim S, Zhan Y et al. Role of intrarenal angiotensin-converting enzyme in nephropathy of type II diabetic rats. *Hypertens Res* 2002; 25: 287–294. [PubMed: 12047045]
15. Ichihara A, Hayashi M, Kaneshiro Y et al. Inhibition of diabetic nephropathy by a decoy peptide corresponding to the “handle” region for nonproteolytic activation of prorenin. *J Clin Invest* 2004; 114: 1128–1135. [PubMed: 15489960]
16. Zhuo JL, Li XC. Novel roles of intracrine angiotensin II and signalling mechanisms in kidney cells. *J Renin Angiotensin Aldosterone Syst* 2007; 8: 23–33. [PubMed: 17487823]
17. Urata H Pathological involvement of chymase-dependent angiotensin II formation in the development of cardiovascular disease. *J Renin Angiotensin Aldosterone Syst* 2000; 1 : S35–S37. [PubMed: 17199219]
18. Graciano ML, Cavaglieri Rde C, Delle H et al. Intrarenal renin-angiotensin system is upregulated in experimental model of progressive renal disease induced by chronic inhibition of nitric oxide synthesis. *J Am Soc Nephrol* 2004; 15: 1805–1815. [PubMed: 15213268]
19. Crackower MA, Sarao R, Oudit GY et al. Angiotensin-converting enzyme 2 is an essential regulator of heart function. *Nature* 2002; 417: 822–828. [PubMed: 12075344]
20. Niimura F, Okubo S, Fogo A et al. Temporal and spatial expression pattern of the angiotensinogen gene in mice and rats. *Am J Physiol* 1997; 272: R142–R147. [PubMed: 9039002]
21. Pohl M, Kaminski H, Castrop H et al. Intrarenal renin angiotensin system revisited: role of megalin-dependent endocytosis along the proximal nephron. *J Biol Chem* 2010; 285: 41935–41946. [PubMed: 20966072]
22. Terada Y, Tomita K, Nonoguchi H et al. PCR localization of angiotensin II receptor and angiotensinogen mRNAs in rat kidney. *Kidney Int* 1993; 43: 1251–1259. [PubMed: 8315939]
23. Matsusaka T, Niimura F, Shimizu A et al. Liver angiotensinogen is the primary source of renal angiotensin II. *J Am Soc Nephrol* 2012; 23: 1181–1189. [PubMed: 22518004]
24. Matsusaka T, Xin J, Niwa S et al. Genetic engineering of glomerular sclerosis in the mouse via control of onset and severity of podocyte-specific injury. *J Am Soc Nephrol* 2005; 16: 1013–1023. [PubMed: 15758046]
25. Kobori H, Ozawa Y, Suzaki Y et al. Enhanced intrarenal angiotensinogen contributes to early renal injury in spontaneously hypertensive rats. *J Am Soc Nephrol* 2005; 16: 2073–2080. [PubMed: 15888567]
26. Gociman B, Rohrwasser A, Lantelme P et al. Expression of angiotensinogen in proximal tubule as a function of glomerular filtration rate. *Kidney Int* 2004; 65: 2153–2160. [PubMed: 15149328]
27. Kobori H, Harrison-Bernard LM, Navar LG. Expression of angiotensinogen mRNA and protein in angiotensin II-dependent hypertension. *J Am Soc Nephrol* 2001; 12: 431–439. [PubMed: 11181790]
28. Schunkert H, Ingelfinger JR, Jacob H et al. Reciprocal feedback regulation of kidney angiotensinogen and renin mRNA expressions by angiotensin II. *Am J Physiol* 1992; 263: E863–E869. [PubMed: 1443118]
29. Navar LG, Satou R, Gonzalez-Villalobos RA. The increasing complexity of the intratubular renin-angiotensin system. *J Am Soc Nephrol* 2012; 23: 1130–1132. [PubMed: 22677556]
30. Gonzalez-Villalobos RA, Seth DM, Satou R et al. Intrarenal angiotensin II and angiotensinogen augmentation in chronic angiotensin II-infused mice. *Am J Physiol Renal Physiol* 2008; 295: F772–F779. [PubMed: 18579707]
31. Schunkert H, Ingelfinger JR, Hirsch AT et al. Evidence for tissue-specific activation of renal angiotensinogen mRNA expression in chronic stable experimental heart failure. *J Clin Invest* 1992; 90: 1523–1529. [PubMed: 1401084]
32. van den Heuvel M, Batenburg WW, Jainandunsing S et al. Urinary renin, but not angiotensinogen or aldosterone, reflects the renal renin-angiotensin-aldosterone system activity and the efficacy of renin-angiotensin-aldosterone system blockade in the kidney. *J Hypertens* 2011; 29: 2147–2155. [PubMed: 21941204]

33. Nishiyama A, Konishi Y, Ohashi N et al. Urinary angiotensinogen reflects the activity of intrarenal renin-angiotensin system in patients with IgA nephropathy. *Nephrol Dial Transplant* 2011; 26: 170–177. [PubMed: 20615910]
34. Nakano D, Kobori H, Burford JL et al. Multiphoton imaging of the glomerular permeability of angiotensinogen. *J Am Soc Nephrol* 2012; 23: 1847–1856. [PubMed: 22997258]
35. Schulz A, Weiss J, Schlesener M et al. Development of overt proteinuria in the Munich Wistar Fromter rat is suppressed by replacement of chromosome 6 in a consomic rat strain. *J Am Soc Nephrol* 2007; 18: 113–121. [PubMed: 17167120]
36. Ichikawa I, Rennke HG, Hoyer JR et al. Role for intrarenal mechanisms in the impaired salt excretion of experimental nephrotic syndrome. *J Clin Invest* 1983; 71: 91–103. [PubMed: 6848563]
37. Matsusaka T, Kobayashi K, Kon V et al. Glomerular sclerosis is prevented during urinary tract obstruction due to podocyte protection. *Am J Physiol Renal Physiol* 2011; 300: F792–F800. [PubMed: 21177778]

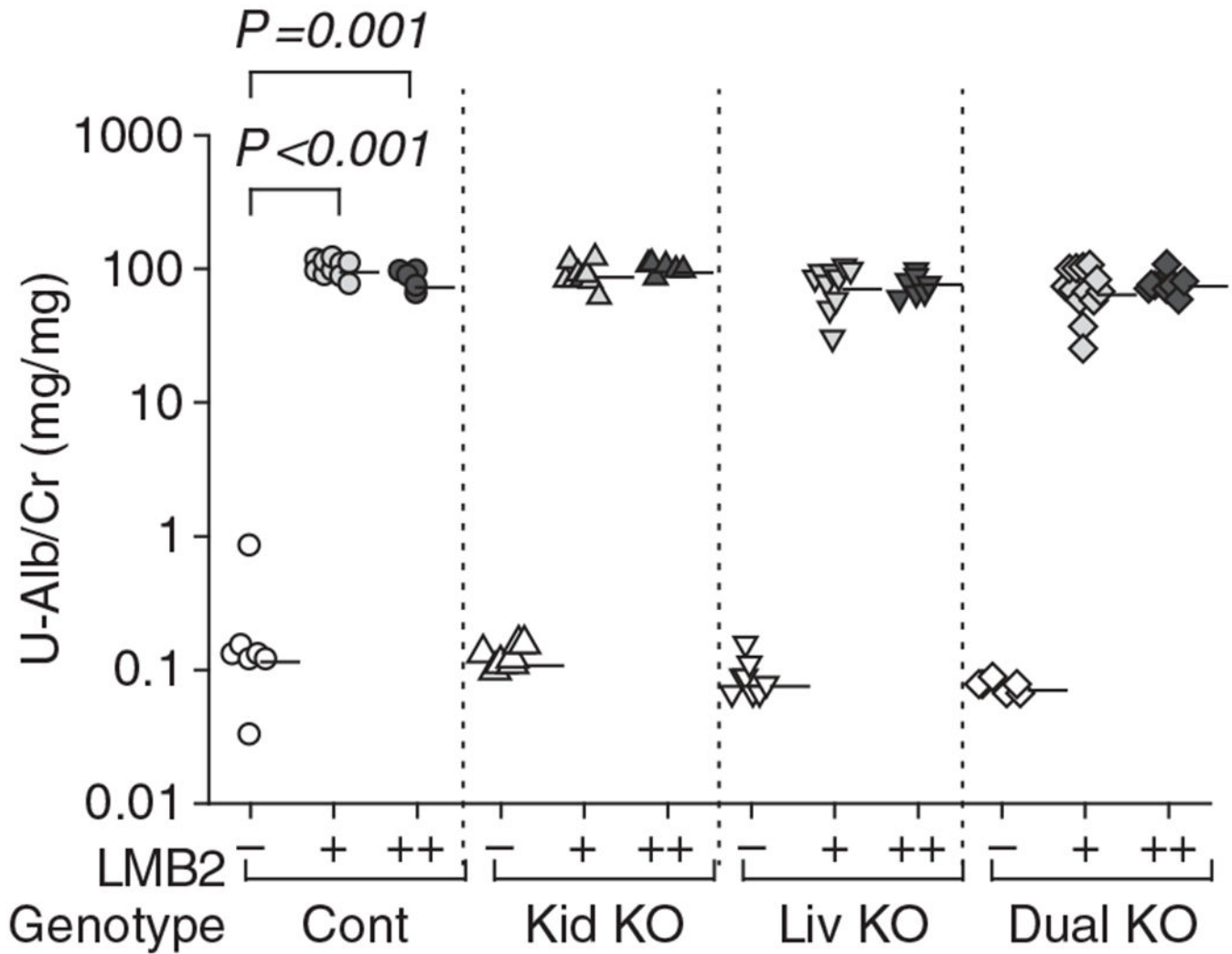


**Figure 1 | Urinary albumin/creatinine ratio (U-Alb/Cr).** NEP25 mice with control *Agt* genotype (Cont), kidney *Agt* knockout (Kid KO), liver *Agt* KO (Liv KO), and dual *Agt* KO (Dual KO) were injected with 1.25 or 2.5 ng per g body weight (BW) of LMB2 (depicted by '+' and '++', respectively) to induce podocyte injury or vehicle (-) and analyzed 7 days later. All types of mice developed massive proteinuria after LMB2 injection. Horizontal bars represent geographical means. The statistical method is described in detail in the legend of Figure 3. For comparison among genotypes at each LMB2 dose, data of Figures 1, 3, 5, and 7a are presented separately for each LMB2 dose in Supplementary Figure S3 online. Representing numerical values are shown in Supplementary Table S3 online.

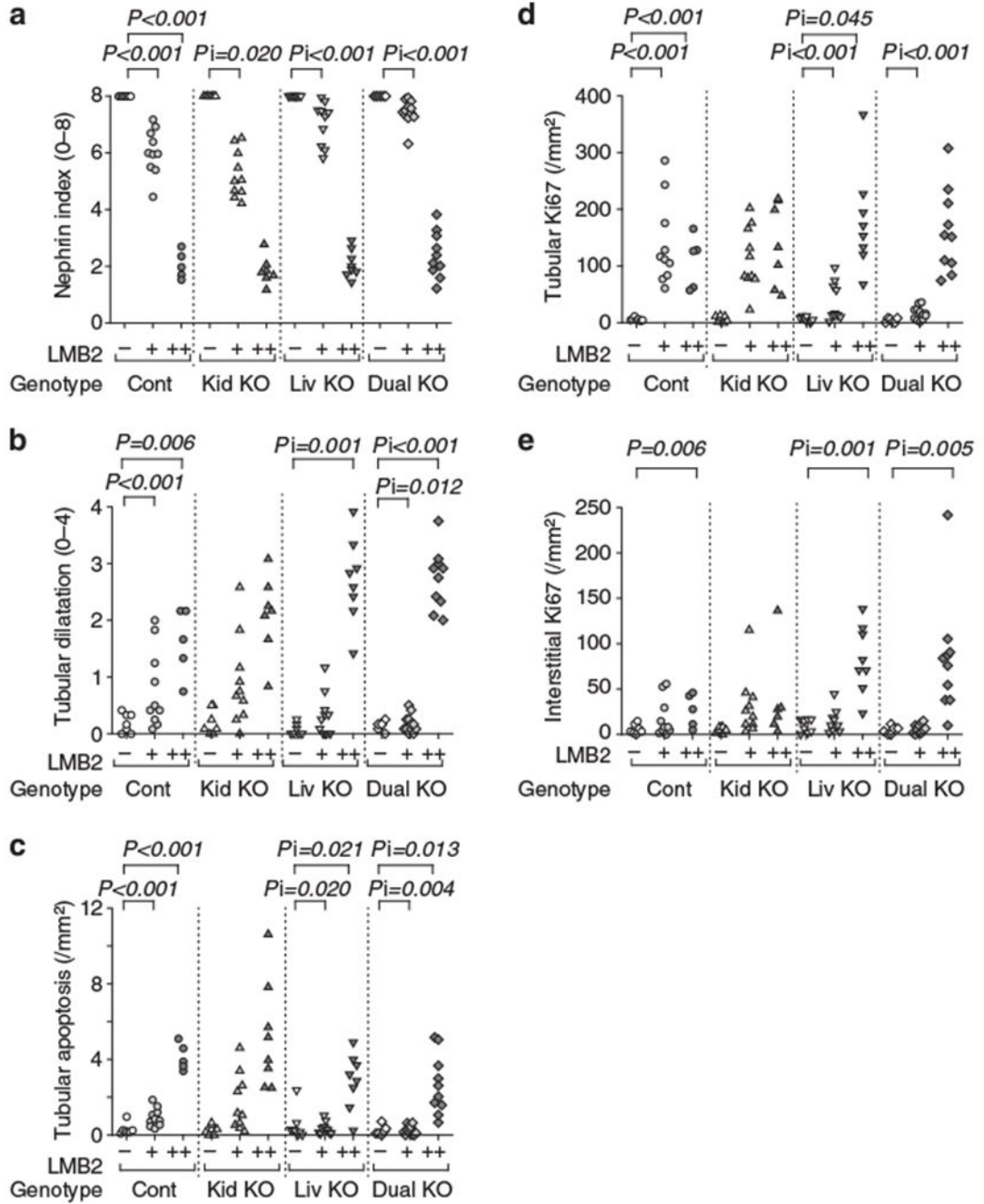


**Figure 2 | Morphometric evaluation.**

(a) Nephryn staining index. LMB2 dose-dependently decreased nephryn index in control mice. After 1.25 ng per g body weight (BW) of LMB2 (+), kidney *Agt* knockout (KO) mice (Kid KO) showed slightly more diminished nephryn, but liver *Agt* KO (Liv KO) and dual *Agt* KO (Dual KO) mice showed more preserved nephryn staining. After 2.5 ng per g BW of LMB2 (++), mice in all genotypes showed uniformly severe nephryn loss. (b) Tubule dilatation. LMB2 induced tubule dilatation similarly in control (Cont) and kidney *Agt* KO mice. In dual *Agt* KO mice after 1.25 ng per g BW of LMB2, tubule dilatation is milder than



that in control mice with the same dose of LMB2. After 2.5 ng per g BW of LMB2, both liver and dual *Agt* KO mice showed more severe dilatation than that in control mice with the same dose of LMB2. (c) Tubule apoptosis. LMB2 induced tubular apoptosis similarly in control and kidney *Agt* KO mice. Liver and dual *Agt* KO mice showed less apoptosis after 1.25 ng per g BW of LMB2, but more apoptosis after 2.5 ng per g BW of LMB2 than that in control mice with the same dose of LMB2. (d) Tubule proliferation (Ki67). LMB2 increased tubular Ki67 similarly in control and kidney *Agt* KO mice. Liver and dual *Agt* KO mice showed less Ki67 after 1.25 ng per g BW of LMB2 than that in control mice with the same dose of LMB2. Liver *Agt* KO mice showed more Ki67 after 2.5 ng per g BW of LMB2 than that in control mice with the same dose of LMB2. (e) Interstitial cell proliferation (Ki67). In control and kidney *Agt* KO mice, 2.5 ng per g BW of LMB2 similarly significantly increased interstitial Ki67. Liver and dual *Agt* KO mice showed more interstitial Ki67 after 2.5 ng per g BW of LMB2 as compared with control mice. The statistical method is described in detail in the legend of Figure 3.

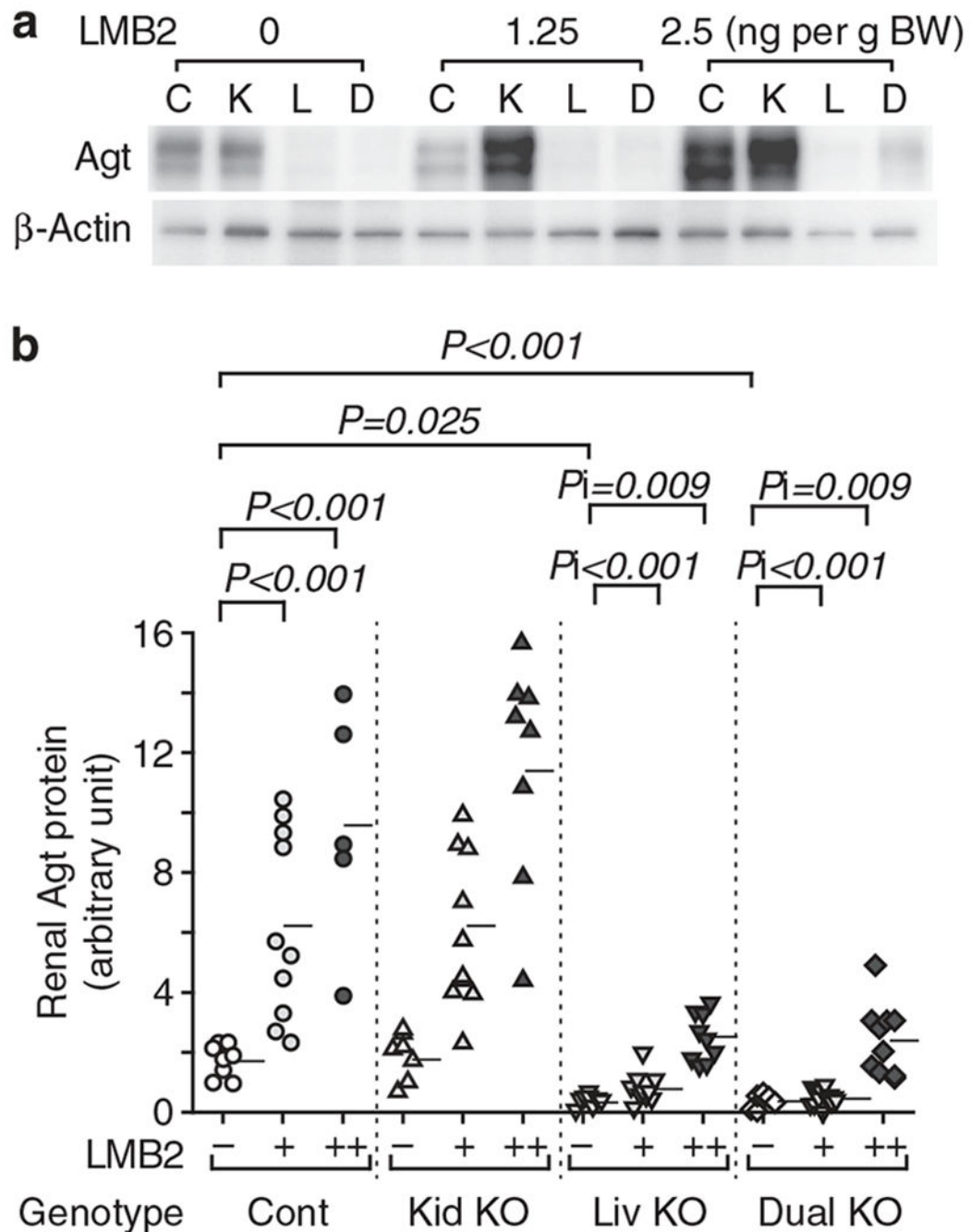


**Figure 3 | Liver- but not kidney-specific *Agt* KO abrogates the increase in renal Agt protein induced by podocyte injury.**

(a) Representative western analysis for renal Agt protein. C, control; D, dual *Agt* knockout; K, kidney *Agt* knockout; L, liver *Agt* knockout. (b) Renal Agt protein content determined by densitometric analysis. Renal Agt protein was increased in control mice dose-dependently after LMB2 injection. Kidney *Agt* KO mice showed similar levels of renal Agt protein to those of control mice both before and after LMB2. Liver and dual *Agt* KO mice had comparably dampened the levels of renal Agt protein before and after LMB2 when

compared with control and kidney *Agt* KO mice. Horizontal bars represent means. Data were analyzed by generalized estimating equation method. Statistical significance for main effects and interaction are shown by *P* and *P*<sub>1</sub>, respectively. Only significant *P* and *P*<sub>1</sub> values are shown. LMB2 1.25 ng per g body weight (BW; +) and 2.5 ng per g BW (+ +) significantly increased *Agt* protein in control *Agt* mice ( $P < 0.001$ ,  $P < 0.001$ ). Without LMB2 (-), liver and dual *Agt* KO mice showed less *Agt* protein than control *Agt* mice ( $P = 0.025$ ,  $P = 0.001$ ). In liver *Agt* KO mice, the increments of *Agt* protein by LMB2 (1.25, 2.5 ng per /g BW) were significantly less than those in control *Agt* mice ( $P < 0.001$ ,  $P < 0.001$ ). Kidney *Agt* KO mice showed similar response to control *Agt* mice, and dual *Agt* KO mice showed similar response to liver *Agt* KO mice.

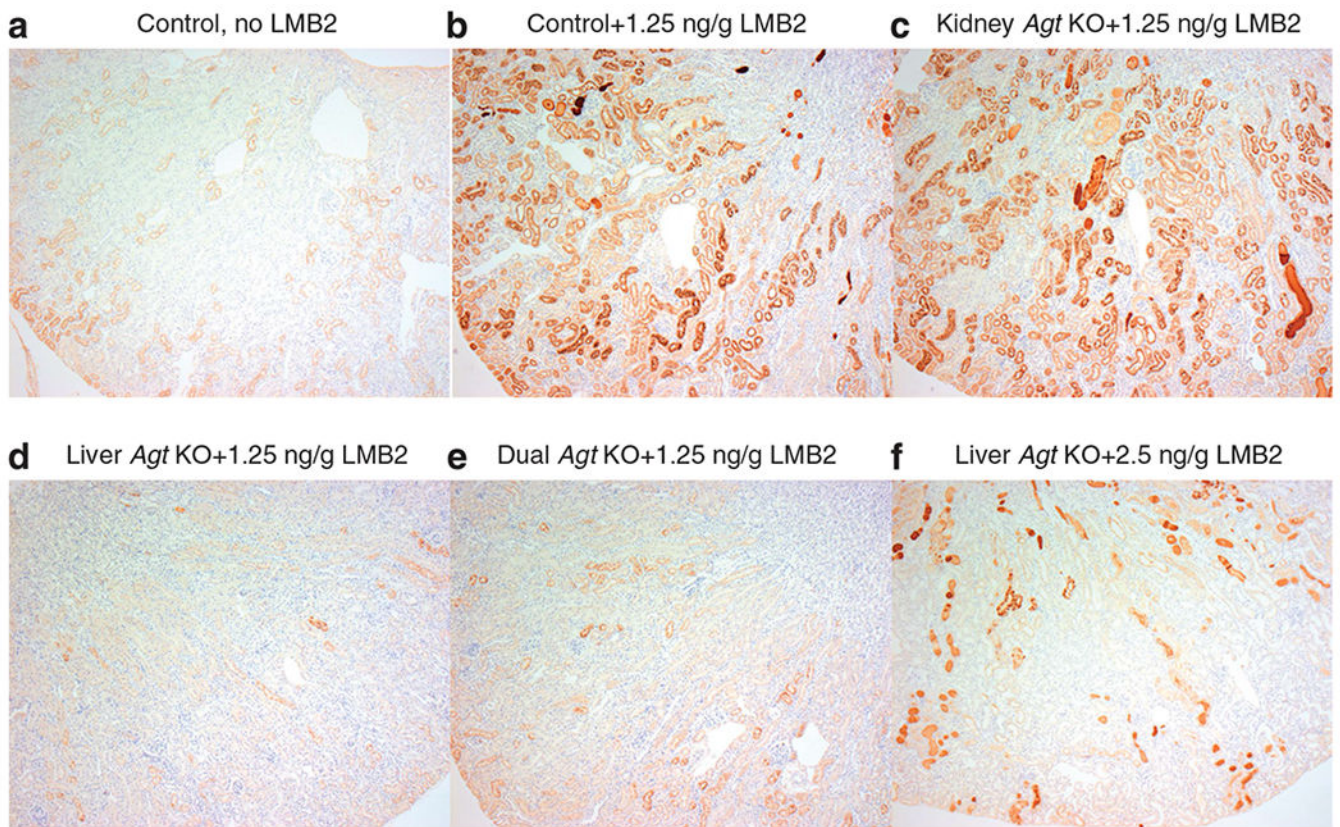


**Figure 4 | Representative pictures for Agt immunostaining.**

Control *Agt* mice (a) showed weak staining mainly in S1 and S2 segments of proximal tubules. After injection of 1.25 ng per g body weight (BW) of LMB2, control *Agt* mice (b) showed intense Agt staining in S1–S3 segments. Kidney *Agt* knockout (KO) mice injected with 1.25 ng per g BW of LMB2 (c) showed intense Agt staining, which is similar to that of control *Agt* mice. In contrast, liver (d) and dual (e) *Agt* KO mice comparably and markedly dampened the otherwise expected heightened Agt staining that followed 1.25 ng per g BW of LMB2. After 2.5 ng per g BW of LMB2, liver *Agt* KO mice (f) showed focal Agt staining along with proteinase casts (original magnification  $\times 50$ ).

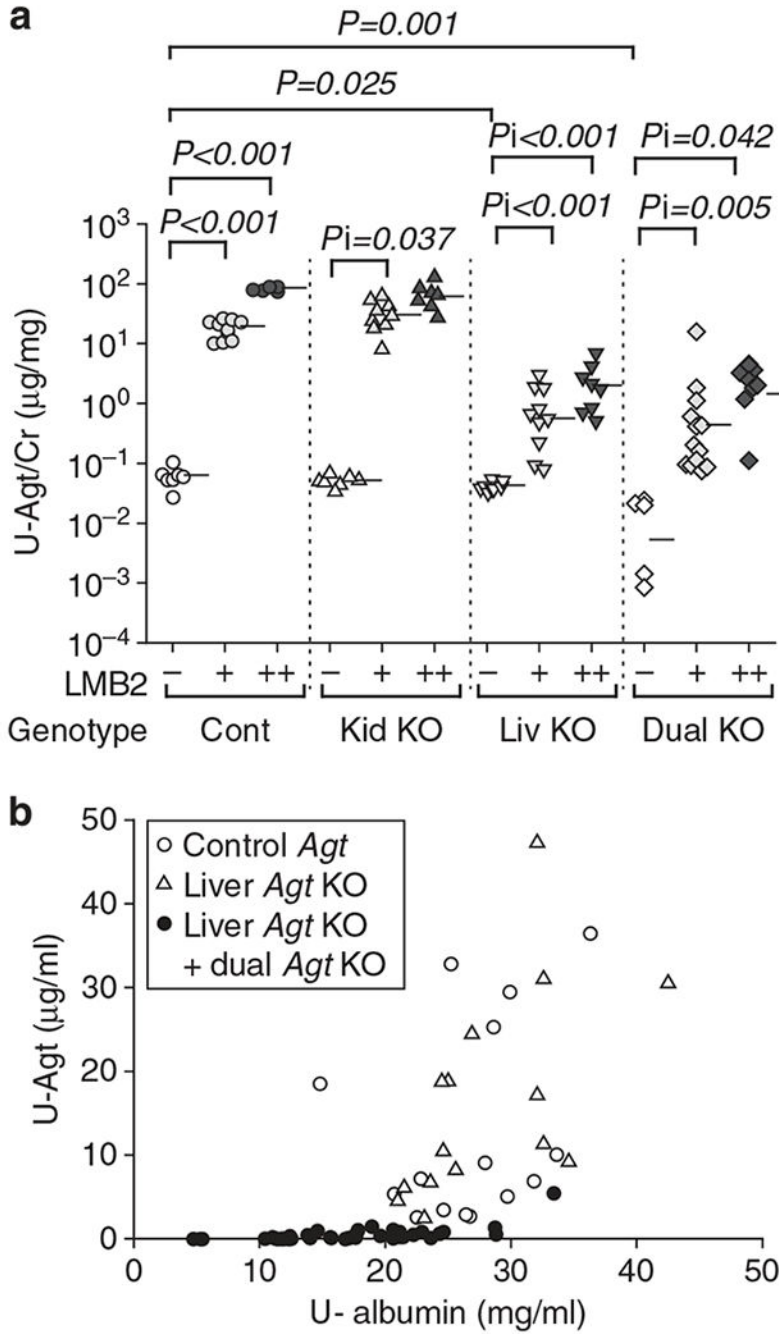


**Figure 5 | Podocyte injury causes massive leakage of liver-derived Agt into the urine.** (a) Urinary Agt/creatinine ratio (U-Agt/Cr). Control (Cont) and kidney *Agt* knockout (KO) mice (Kid KO) showed similar dose-dependent increase in urinary Agt/Cr ratio after LMB2. Liver *Agt* KO (Liv KO) and dual *Agt* KO (Dual KO) mice showed significantly attenuated urinary Agt/Cr ratio when compared with control and kidney *Agt* KO mice for the same dose of LMB2. Previously, we found that kidney *Agt* KO showed lower urinary Agt at baseline than control mice. In this study, this was not reproduced probably because of the limited number of mice. Horizontal bars represent geographical means. (b) Correlation

between U-Agt and albumin concentration. In control (represented by open circles) and kidney *Agt* KO mice (open triangles) injected with either dose of LMB2, a significant correlation exists between urinary albumin and Agt concentration ( $r = 0.399$ ,  $P = 0.029$ ). Of note, liver and dual *Agt* KO mice (closed circles) showed uniformly low urinary Agt irrespective of urinary albumin levels.

Author Manuscript

Author Manuscript

Author Manuscript

Author Manuscript



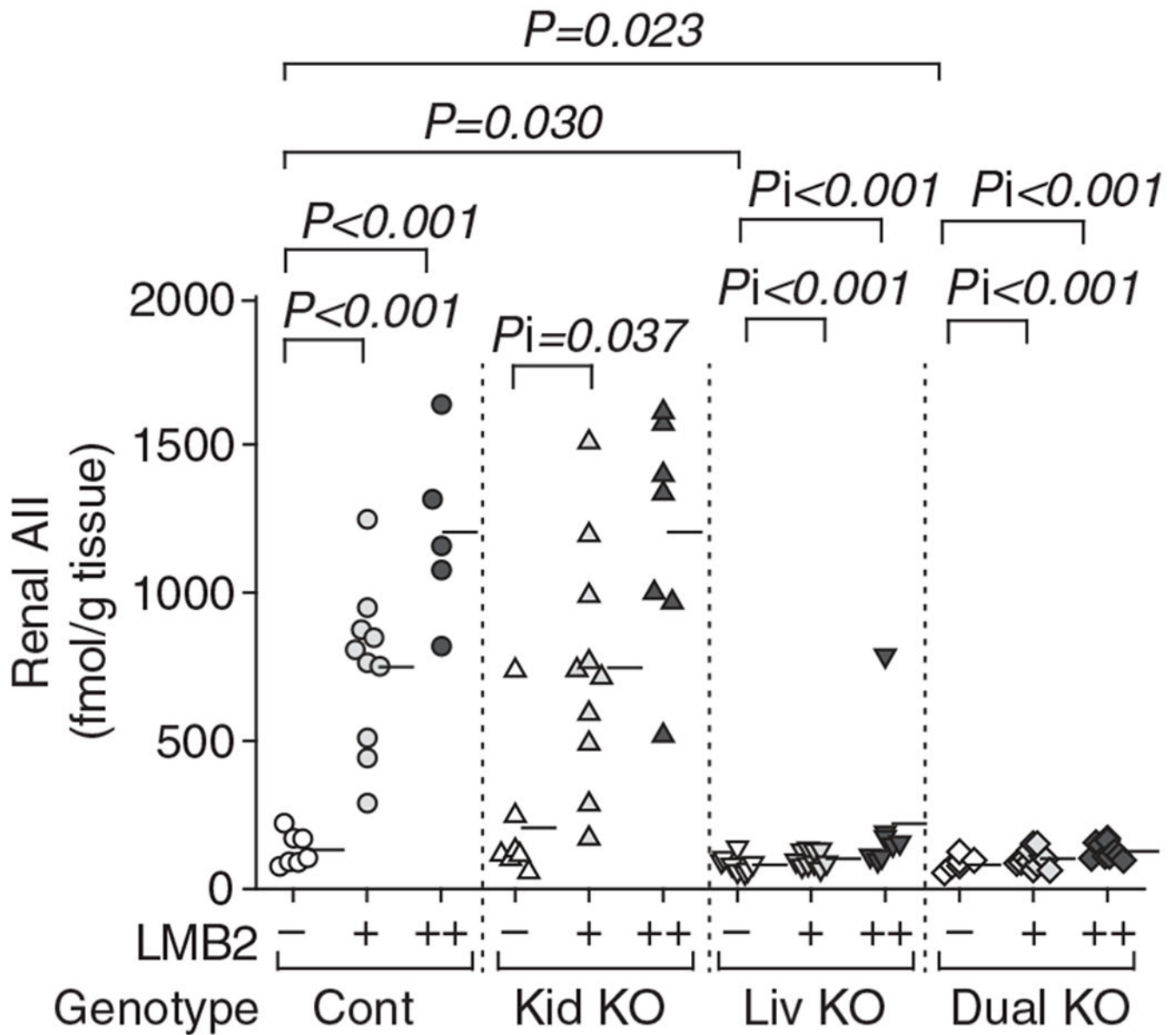


**Figure 6 | Liver- but not kidney-specific *Agt* KO abrogates the increase in renal angiotensin II (AII) induced by podocyte injury.**

Control (Cont) and kidney *Agt* knockout (KO) mice (Kid KO) showed dose-dependent increase in renal AII after LMB2 in a similar manner. In contrast, both liver *Agt* KO (Liv KO) and dual *Agt* KO (Dual KO) mice uniformly showed low renal AII both before and after LMB2. One liver *Agt* KO mouse injected with 2.5 ng per g body weight (BW) of LMB2 showed exceptionally high renal AII. The level of renal *Agt* mRNA in this mouse was not elevated, and was lower than the average value of control *Agt* mice without LMB2. Horizontal bars represent means.

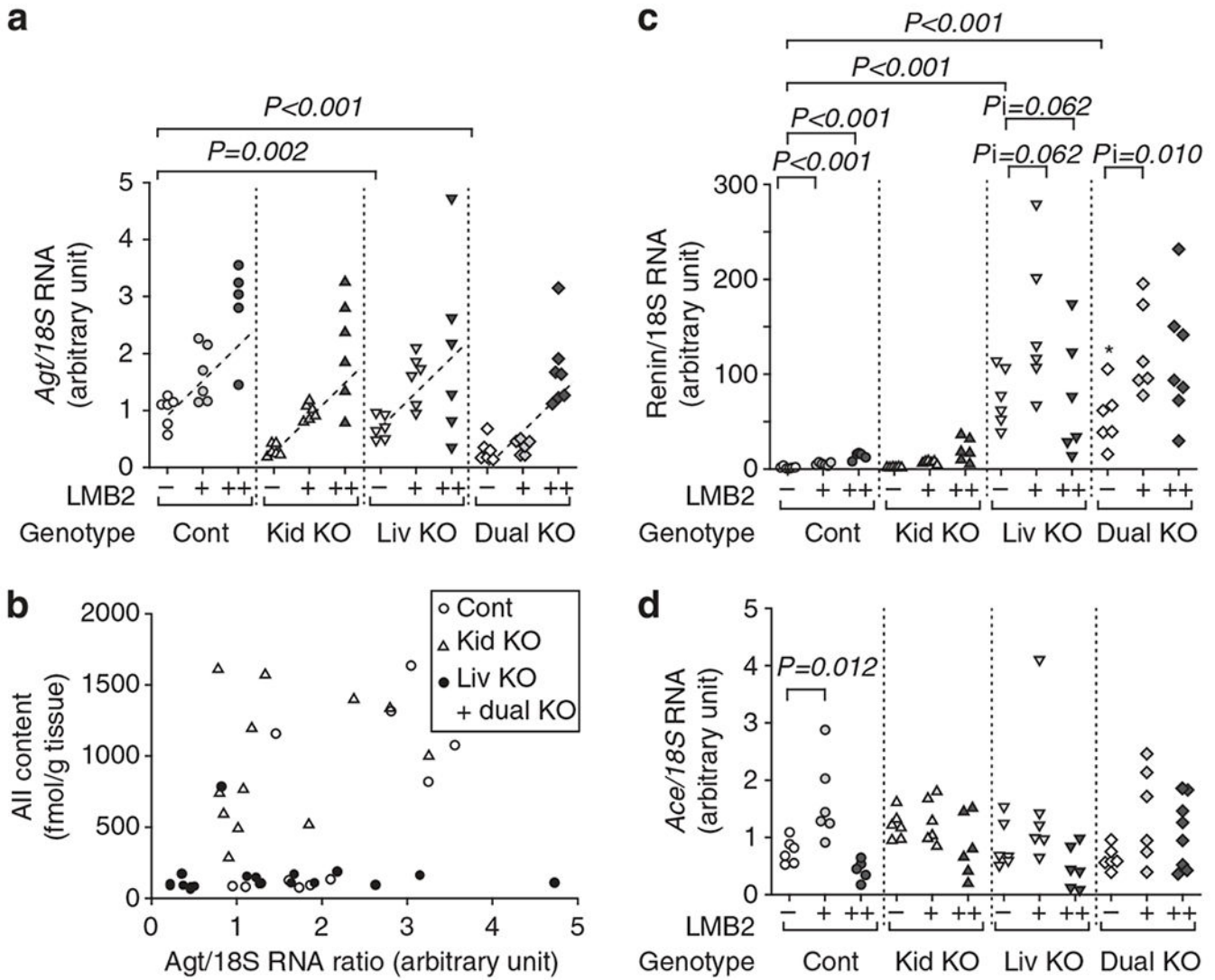


**Figure 7 | Podocyte injury induces a small increase in renal *Agt* mRNA that is not correlated with renal angiotensin II (AII).**

(a) Renal *Agt* mRNA/18S rRNA (*Agt*/18S RNA) ratio. In each genotype, LMB2 increased *Agt*/18S RNA dependently on the LMB2 dose with a similar slope. Without LMB2, kidney *Agt* knockout (Kid KO) and dual *Agt* KO (Dual KO) mice had less *Agt*/18S RNA than control *Agt* (Cont) mice. Consequently, kidney and dual *Agt* KO mice given 1.25 ng per g body weight (BW) of LMB2 showed lower *Agt*/18S RNA than control *Agt* mice given the same dose of LMB2. Liver *Agt* KO (Liv KO) mice showed a pattern similar to that of control *Agt* mice. Graphs expressing data for each LMB2 dose are presented in Supplementary Figure S3 online. (b) Relationship between renal *Agt* mRNA and angiotensin II (AII) content after injection of LMB2. In liver and dual *Agt* KO mice (closed circles), AII content was uniformly low regardless of the *Agt* mRNA level. In contrast, control (open circles) and kidney *Agt* KO (open triangles) mice showed high AII content, which was not associated with renal *Agt* mRNA ( $r = 0.330$ ,  $P = 0.124$ ). (c) Renal renin mRNA/18S rRNA (renin/18S RNA) ratio. Without LMB2, liver and dual *Agt* KO mice

showed markedly higher renal renin/18S RNA than control mice. LMB2 injection slightly increased renin/18S RNA in control *Agt* KO mice. Kidney *Agt* KO mice showed a pattern similar to that of control mice. Increments of renin/18S RNA by LMB2 in liver and dual *Agt* KO mice were more than those in control mice. These changes are not in parallel with the renal AII content. Renal *Ace* mRNA/18S rRNA (*Ace*/18 S RNA) ratio. (d) Renal *Ace* mRNA was not affected by LMB2 injection in any of the *Agt* genotypes, and there was no significant difference among *Agt* genotypes, except for a small increase by 1.25 ng per g body weight (BW) of LMB2 in control mice.

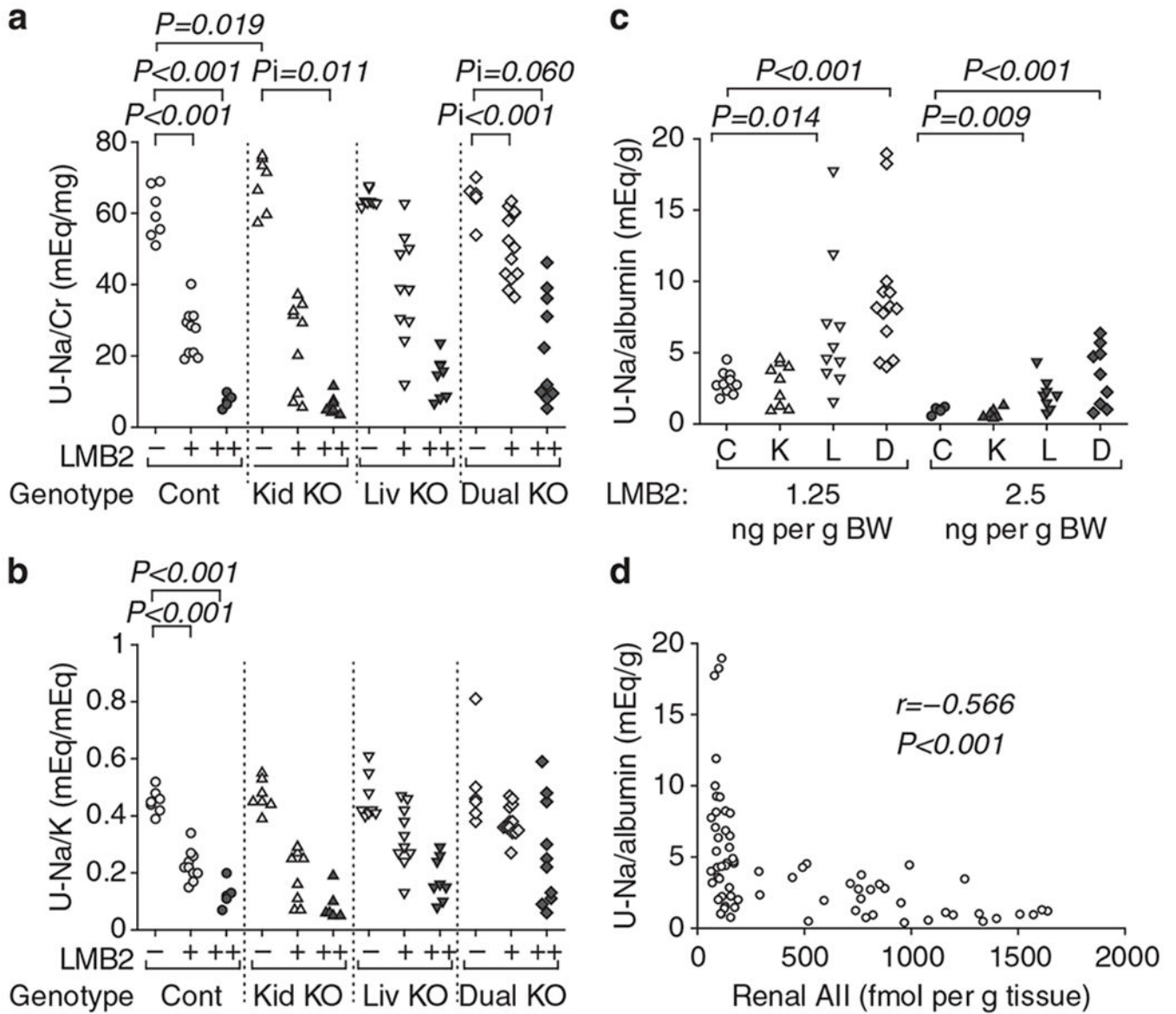


**Figure 8 | Liver *Agt* knockout (KO) attenuates sodium (Na) retention after podocyte injury.** Control (Cont) and kidney *Agt* KO (Kid KO) mice showed dose-dependent decreases in (a) urinary sodium/creatinine (Na/Cr) and (b) sodium/potassium (Na/K) ratios after LMB2 injection. (c) Liver *Agt* KO (Liv KO) and dual *Agt* KO (Dual KO) mice injected with LMB2 showed significantly higher urinary Na concentration normalized by urinary albumin concentration than control mice. (d) In all genotypes of mice injected with LMB2, urinary Na/albumin ratio was inversely correlated with renal angiotensin II (AII) content ( $R = -0.566$ ,  $P < 0.001$ ).